Technologia i Automatyzacja Montażu

Volume 120, Issue 2/2023, Pages 19-32
https://doi.org/10.7862/tiam.2023.2.3

Original Research

SELECTION OF MATERIALS FOR REPAIRING PUNCTURES OF METAL SKIN OF SEMI-MONOCOQUE STRUCTURES USING COMPOSITE PATCHES

DOBÓR MATERIAŁÓW DO NAPRAW PRZEBIĆ POKRYĆ METALOWYCH STRUKTUR PÓŁSKORUPOWYCH Z ZASTOSOWANIEM ŁAT KOMPOZYTOWYCH

Jan GODZIMIRSKI[1], Marek ROŚKOWICZ[1], Iga BARCA[1,*]

[1] Faculty of Mechatronics, Armament and Aerospace, Military University of Technology, Sylwester Kaliski Street 2, Warsaw, Poland

* Corresponding author: iga.barca@wat.edu.pl

Abstract

For repairing punctures of skin of semi-monocoque structures under field conditions, simple methods are sought to guarantee the reliability of the repaired structure. Therefore, adhesive joints and composite materials are being increasingly used in repairs. During repairs using adhesion, an important aspect that affects the quality of the joint is the selection of the adhesive and the quality of surface preparation of the parts to be joined. This is necessary to get the right bond strength and durability of the joint in working environments characterized by extreme temperatures and exposure to chemicals and moisture. The purpose of the study was to select an adhesive with good strength properties for bonding AW2024T3 aluminum sheets to carbon and glass composites, and to analyze the effect of metal surface preparation on the strength of adhesive joints (grinding, sandblasting and chemical surface preparation). The tests were carried out on overlap (metal-composite) specimens. For selected adhesives, strength tests were also carried out on specimens replicating the repaired damage with a diameter of 20 mm of metal skin repaired by different methods, including composite patches and adhesive joints. The specimens were loaded in tension and loss of stability. The tests made it possible to determine the requirements for composite patches used for repairing upper and lower airframe wing skins.

Keywords: repair node, adhesive joints, surface roughness, composite materials, numerical analysis.

Streszczenie

Do napraw przebić pokryć konstrukcji półskorupowych w warunkach polowych, poszukuje się prostych metod, które zagwarantują niezawodność naprawianej struktury. Dlatego coraz częściej w naprawach wykorzystuje się połączenia adhezyjne i materiały kompozytowe. Podczas napraw z zastosowaniem klejenia ważnym aspektem, który wpływa na jakość połączenia, jest dobór odpowiedniego kleju oraz jakość przygotowania powierzchni klejonych elementów. Jest to niezbędne do uzyskania odpowiedniej siły wiązania i trwałości połączenia w środowisku pracy, które cechują ekstremalne temperatury oraz narażenie na działanie chemikaliów i wilgoci. Celem badań był dobór kleju o dobrych właściwościach wytrzymałościowych do łączenia blach AW2024T3 z kompozytami węglowymi i szklanymi oraz analiza wpływu przygotowania powierzchni metalowych na wytrzymałość połączeń adhezyjnych (szlifowanie, piaskowanie i chemiczne przygotowanie powierzchni). Badania przeprowadzono na próbkach zakładkowych (metalowo-kompozytowych). Dla wybranych klejów wykonano również badania wytrzymałościowe próbek imitujących naprawione uszkodzenie o średnicy 20 mm pokrycia metalowego naprawianego różnymi metodami, w tym z zastosowaniem łat kompozytowych i połączeń adhezyjnych. Próbki obciążano na rozciąganie i utratę stateczności. Przeprowadzone badania pozwoliły określić wymagania dotyczące łat kompozytowych stosowanych do napraw górnych i dolnych pokryć skrzydeł płatowców.

Słowa kluczowe: węzeł naprawczy, połączenia klejowe, chropowatość powierzchni, materiały kompozytowe, analiza numeryczna.

1. Introduction

Despite the use of new materials in aircraft manufacturing, the skin of aircraft in service is still made of aluminum alloys [1]. Research is constantly being carried out on the most favorable solutions for repairing defects in primary aircraft structures, including skins, which are most often damaged during operation [2]. The conventional approach to maintaining aircraft structures can be divided into four phases: detection of defects, diagnosis of their nature, prediction of their future behavior and implementation of countermeasures including repairs [3]. With such an approach, it is required to develop and design optimal repairs and evaluate their durability. Repairs to such structures involve cutting a hole to remove the damaged material, placing an insert to fill the hole and attaching a closing patch to support the damaged airframe structure [4].

Two methods of repairing skins are used: using adhesive joints when using composite patches, or using mechanical joints when using metal patches [5]. Due to weight savings [6], the use of classical mechanical fasteners (rivets, screws) to connect composite elements is increasingly minimized, as they cause stress concentrations at the holes [7, 8, 9]. Bonding is one of the most suitable joining technologies in terms of weight reduction and mechanical properties [10]. Adhesive repairs of the secondary bonding type (secondary bonding - joining two cured parts together using a structural adhesive) using certified high-strength epoxy adhesives for repairing aerospace structures, i.e. Loctite 9394 Aero [11], have great potential. Secondary bonding is a comprehensive bonding method because it provides faster assembly, easier handling, lower production costs and provides flexibility in the production cycle. The strength of adhesive bonds used in repairs, among other things, is affected by three main parameters - the type of adhesive selected, the material of the patch and the quality of surface preparation.

In order to make an effective adhesive bond, an optimized bonding system, i.e., the selection of appropriate parameters of substrate/surface/pretreatment/adhesive/primer combination must be selected [12]. The quality of the adhesive bond depends very much on the surface preparation strategy used for joining [13, 14]. The quality of the surface affects the mechanical properties of the interphase adhesion [15]. The mechanical properties of adhesive joints are also influenced by environmental factors such as air humidity, joint working temperature, joining process and curing cycle parameters [16]. Due to the reactivity of freshly prepared surfaces and the proximity and activity of contaminants in the environment, cleaning these surfaces sufficiently to achieve reliable adhesive bonds can be particularly difficult under field conditions [17]. The most commonly used method of surface preparation under field conditions is grinding using specialized abrasive fabric for metal surfaces [18]. Metal surfaces require more surface treatment than composite materials and most often have poor interphase adhesion mechanical properties, which can be a reason for damage initiation [19].

During repairs, a patch is bonded to restore the primary strength of the damaged structure. For this purpose, patches made of carbon or glass composites infused with epoxy resin are used [20]. They are usually laid in such a way as to achieve quasi-isotropic characteristics, which is extremely important in the repair of aircraft structures [21]. In addition, the material parameters must be properly selected so that the repair node is characterized by sufficient strength. Also important is the condition of local "not stiffening" of structural elements as a result of the repairs performed, as this can cause additional stresses around the repair node [22, 23] and cause additional stress concentrations in the adhesive bond [24].

The purpose of the study was to determine the effect of surface preparation on the strength of secondary bonding when joining metal parts made of EN AW-2024-T3 aluminum alloy and composite parts made of CFRP and GFRP composites. In addition, the selection of the most favorable geometric parameters of patches when repairing metal structures and different methods of metal surface preparation were analyzed, using patches made of GFRP composite with different thicknesses. There is little research on secondary bonding using composite overlays made of fabrics infused with epoxy resin, mainly studies are performed on prepregs. Above that, an analysis was made of modern methods of surface preparation for bonding using the most advanced methods applicable in the industry, using chemical surface preparation.

2. Experimental studies

The purpose of the study was to determine the effect of surface preparation on the strength of adhesive joints, and to select the most favorable technological repair parameters (surface preparation method and patch geometry).

2.1. Overlap specimens - adhesive selection and surface preparation methods

The first part of the study was the selection of an adhesive for the repairs. Tests were carried out on metal-composite overlap specimens 20x12,5x2 mm (width/length/thickness) (Fig.1) made of EN AW-2024-T3 aluminum alloy and carbon/glass fiber-reinforced composites (CFRP and GFRP). The carbon

composite used is GG204T 2 x 2 Twill 3K fabric in the form of prepreg saturated with IMP503 46 epoxy resin.

The glass composite, on the other hand, is a 110g/m2 fabric saturated with L285/H285 epoxy resin. Four adhesives were used for the bonding overlap specimens: L285/H285 (aerospace certificate resin), Epidian 57/Z1, DP420 and Loctite 9464. The characteristics of the adhesives are shown in the Table 1. All adhesives are two-component, they were mixed on a Teflon plate at room temperature in proportions according to the manufacturer's instructions (Table 1). After mixing, the adhesives were applied with a sterile wooden stick.

Table 1. Characteristics of the used adhesive

Adhesive name	Resin - chemical type	Hardener - chemical type	Mass ratio (resin/hardener)	Course of curing	Shear strength [N/mm^2]	Peel strength [N/mm]
L285/H285	Epoxy	Amine	100:40	24h at 23°C + 15h at 60°C	-	-
Epidian 57/Z1	Epoxy	Amine	100:10	24h at 23°C + 5h at 80°C	15.0	-
Loctite 9464	Epoxy	Amine	1:1	3 days at 23°C	18.2	7.00
DP420 3M	Epoxy	Amine	2:1	24h at 23°C	31.0	8.76

Before bonding, in first part of tests the joined surfaces of the specimens were washed with extraction gasoline then grinded with 3M abrasive fabric number 80 using a pneumatic gun at 1000 rpm for 60 seconds, designed for aluminum surfaces, and then washed with extraction gasoline. Threads were used to obtain a 0.15-mm-thick adhesive layer. The tool shown in the figure 2 was used to obtain adhesive layer with the same overlap lengths of 12.50 mm. All specimens were loaded equally at the same time with a force 1.2 MPa. In each case, the manufacturer's recommended process was used to cure the adhesive. The specimens were subjected to tensile testing on a testing machine and the results are shown in Table 2. Confidence intervals were also determined using the Student's t method (1)(2) - Figure 3.

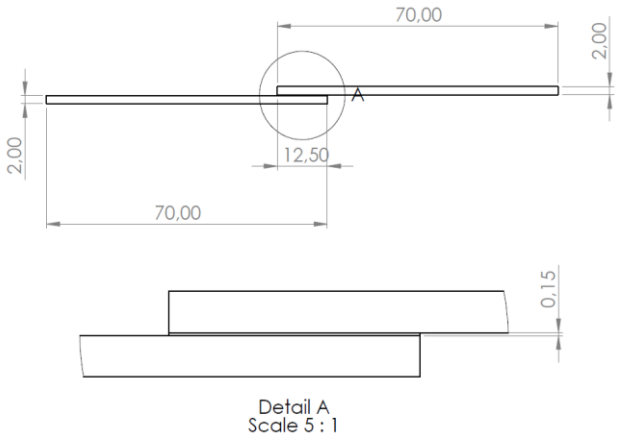

Fig.1. Geometric dimensions of lap specimens

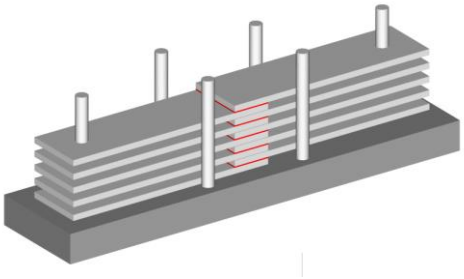

Fig. 2. The tool in which the specimens were placed in order to obtain a given weld length

$$n = 6 - number\ of\ specimens$$

$$\bar{X} = \frac{\sum_{i=1}^{n} n_i}{n} \quad (1)$$

$$SD = \sqrt{\frac{\sum_{i=1}^{n} {n_i}^2 - \bar{X}^2}{n * (n-1)}} \quad (2)$$

$$t_\alpha = 2{,}571 - Student's\ t - ratio\ for\ 6\ specimens$$

$$TS = SD * t_\alpha \quad (3)$$

The joints prepared with 3M's DP420 adhesive had the highest load capacity.

In order to determine the surface preparation method that provides the highest load capacity for the joint, additional tests were carried out for aluminum-carbon lap specimens. The adhesive that had the highest shear strength in previous tests was used. Two additional methods of surface preparation for bonding were tested: sandblasting (using F80 electrocorundum grains at an operating pressure of 8 at. And cleaning before and after with extraction gasoline), and grinding and using a primer (Surface pre-treatment

Table 2. Load capacity of overlap joints for different thermoplastics materials

Specimen no.	Load capacity [N]							
	AW 2024T3-CFRP				AW 2024T3-GFRP			
	L285/H285	Epidian 57/Z1	DP420	Loctite 9464	L285/H285	Epidian 57/Z1	DP420	Loctite 9464
1	1351	2253	3718	3000	871	2395	3463	3000
2	983	2240	3487	2850	846	2640	2197	2659
3	1185	1795	3852	3000	1641	2715	3378	2210
4	1113	1937	2805	2590	684	1709	2336	2252
5	1523	1493	3497	2790	493	3082	2480	2694
6	760	1429	3280	-	795	2702	1797	-
Average load capacity	1152±282	1858±372	3440±387	2846±212	888±413	2540±486	2608±590	2563±410

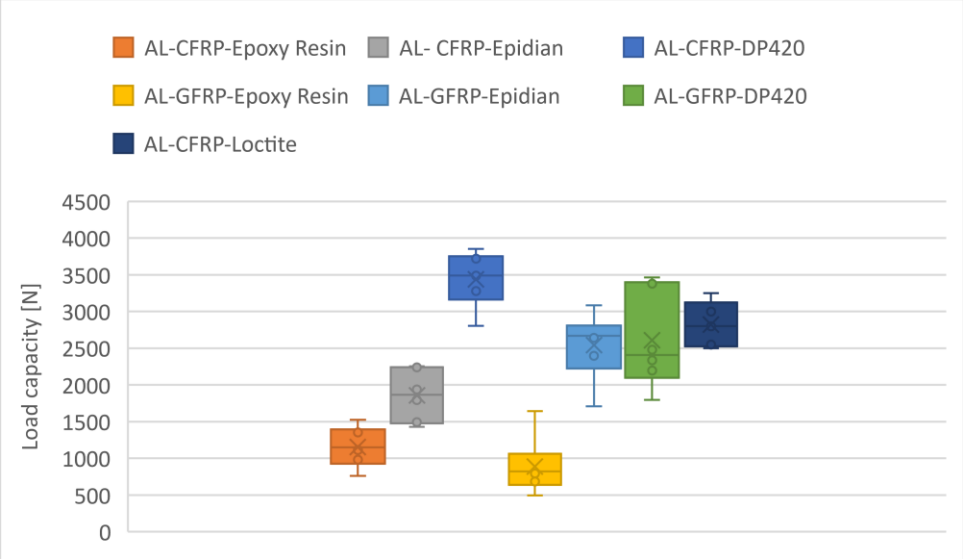

Figure 3. Arithmetic averages of overlap joints load capacity

AC-130-2 Kit from 3M). The two-component primer was mixed at a volume ratio of 49.2:1 ml. After mixing it for 60 s and leaving it for 30 min, it was applied to the grinded and cleaned surface (extraction gasoline) with a brush. It was left on the surface for 5 min, according to the manufacturer's instructions. The samples were then bonded together after 60 min after evaporation of the product. The results of the overlap joint load capacity tests are shown in Table 3. Confidence intervals were also determined - Figure 4.

Table 3. Bearing capacity of overlap joints for different surface preparation methods

Specimen no.	AW 2024T3-CFRP		
	DP420		
	Grinding	Sandblasting	Grinding + Primer
1	3718	6180	6387
2	3487	5425	6917
3	3852	5507	5820
4	2805	6050	5485
5	3497	5853	6103
6	3280	5990	5773
Average Load capacity [N]	3440.00±387.00	5834,17±320.18	6080.83±537.50

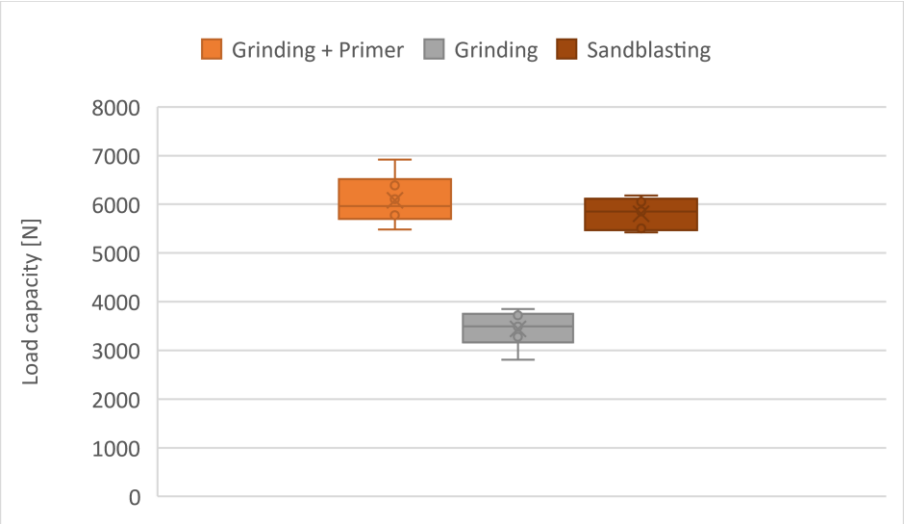

Figure 4. Arithmetic averages of overlap joints load capacity

The use of primer for surface preparation increased the load capacity of the joint by about 57%. An example of a damaged specimen after testing is shown in figure 5. In each case, the composite was damaged by delamination.

Specimens whose surfaces were grinded before bonding and treated with primer at the same time have the highest load capacity.

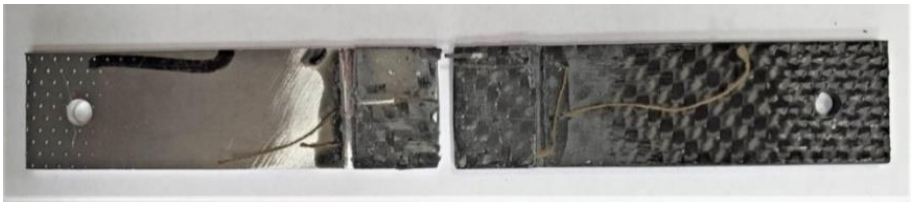

Fig. 5. The specimen after the strength test

2.2. Specimens with a hole - the effect of patch thickness and surface preparation on the strength of overlay joints

Tests in this field were carried out for aluminum (AW 2024T3) specimens with a laser-cut hole (the hole was assumed to be equivalent to the damage to the skin) with the dimensions shown in Figure 6. The specimens were in the form of overlay joints with a circular composite patch (GFRP 110 g/m2) with a diameter of 70 mm and three different thicknesses (1 mm, 1.6 mm and 2 mm) and quasi-isotropic properties. Three specimens were prepared for each surface preparation method and patch thickness. A 19.9 mm diameter insert made of aluminum alloy was placed in the hole. In this case also, three methods of surface preparation were used: grinding, grinding + primer and sandblasting. The specimens were subjected to tension on an MTS series 809 tensile machine - Table 4 – the results were averaged. The undamaged and damaged specimen (without repair) were also tested.

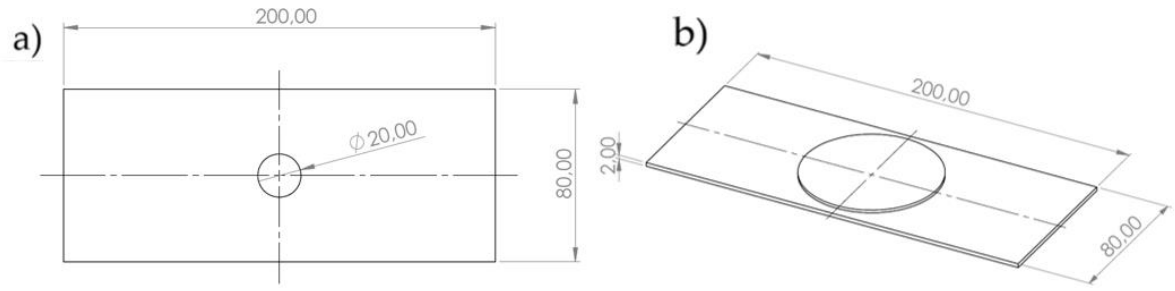

Fig. 6. Geometric dimensions of: a) the plate with a hole, b) repaired specimens

Table 4. Static test results for specimens with repair node

Specimen no.	Kind of specimen	Thickness	Method of Surface preparation	Force [kN]
1	Undamaged	-	-	69,3
2	Damaged	-	-	50
3	Repaired	1 mm	Grinding	49,5
4			Grinding + Primer	51,5
5			Sandblasting	52
6		1.6 mm	Grinding	61,5
7			Grinding + Primer	61,5
8			Sandblasting	60
9			Sandblasting + primer	62,5
10		2 mm	Grinding	58
11			Grinding + Primer	63,5
12			Sandblasting	59

Figure 7 shows examples of patch failure for different thicknesses (1 mm, 1.6 mm and 2 mm) for specimens whose surfaces were grinded before bonding and then primer was applied. In the case of the specimen with a 1 mm thick patch, it cracked together with the specimen (a). The specimen with a 1.6-mm-thick patch cracked and then loaded the patch, which partially disrupted (b). On the other hand, the specimen with a 2-mm-thick patch experienced delamination of the composite overlay during specimen cracking (c).

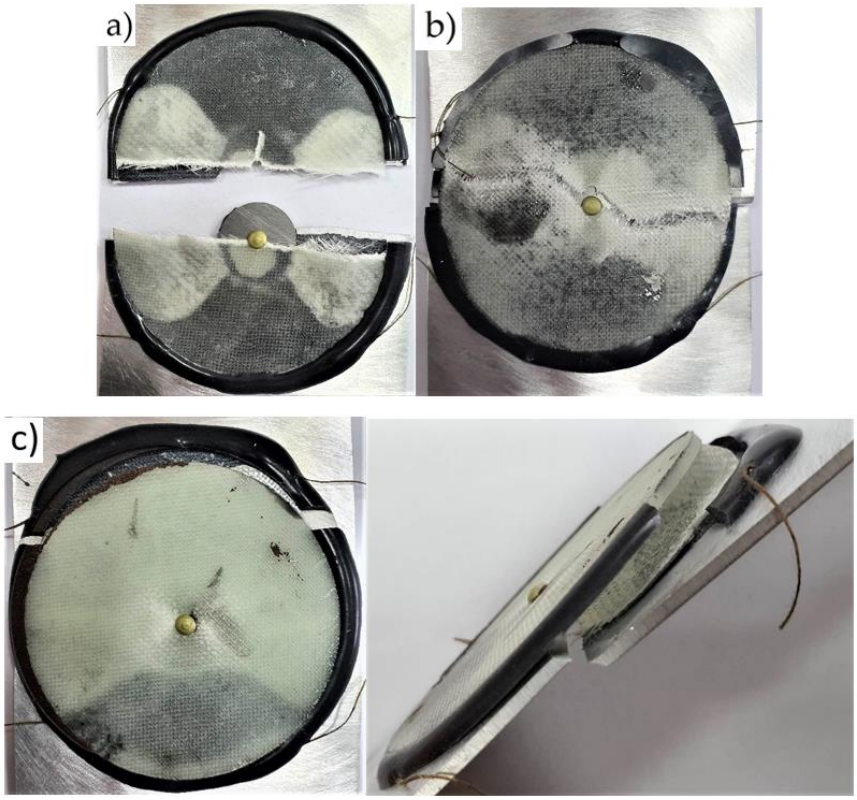

Fig. 7. Examples of patch damage during testing: 1 mm (a),1.6 mm (b), 2 mm (c)

The use of primer increased the strength of the applied joint by only about 4%. The highest strength was characterized by specimens that used 2 mm thick overlays with a surface prepared by grinding and primer. In neither case was adhesive failure observed - detachment of the patch from the repaired surface.

2.3. Surface roughness

In order to check the effect of the primer (AC-130--2 Surface Pretreatment Kit) on the geometric parameters of the surface of the aluminum sheet under study, the surface roughness was measured using a VHX-6000 Keyence optical microscope, at 500x magnification, and five specimens whose surfaces were prepared using five methods (Figure 8).

Figures 9-11 show the surfaces of the prepared specimens without primer (a) and with (b).

Fig. 8. Surface roughness test specimens prepared by the following methods (from left): primer, grinded, grinded + primer, sanded, sanded + primer

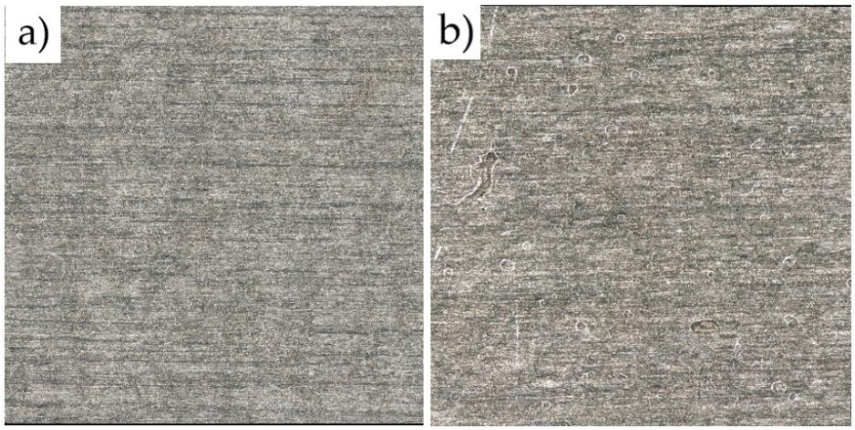

Fig. 9. The surface of the specimen without surface preparation (a) and after using primer (b)

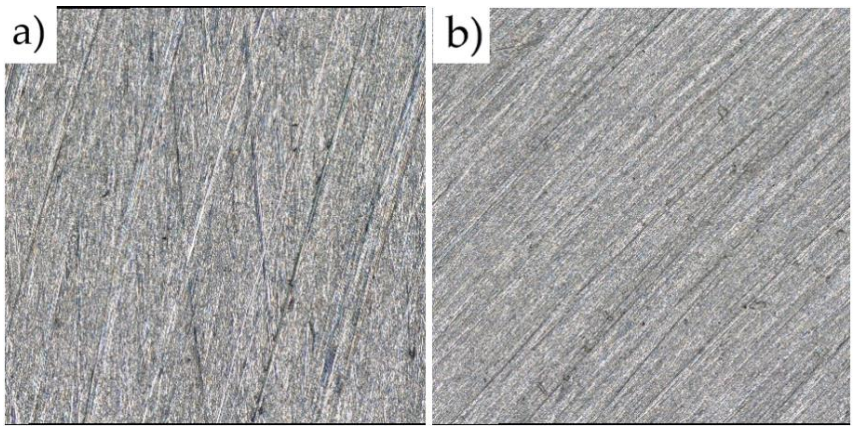

Fig. 10. Surface grinded with abrasive cloth No. 80 from 3M (a) and sanded and washed with primer (b)

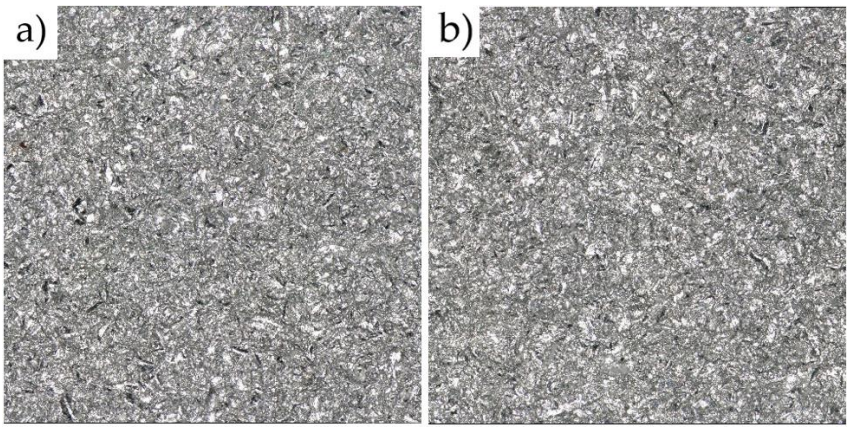

Fig. 11. Surface grinded with abrasive fabric No. 80, 3M (a) and grinded and washed with primer (b)

Surface roughness measurements were also carried out on an optical microscope for all specimens shown in the figures. Two measurements were taken for each surface preparation method. Four parameters were measured, using two methods: measurement on the line- R (Fig. 12); measurement on the surface - S (Fig. 13):

- Ra - the arithmetic mean deviation of the profile from the mean line,
- Rz - surface roughness according to the five points of the profile on the line,
- Sa - arithmetic mean deviation of the profile from the mean plane,
- Sz - surface roughness according to five points of the profile on the plane.

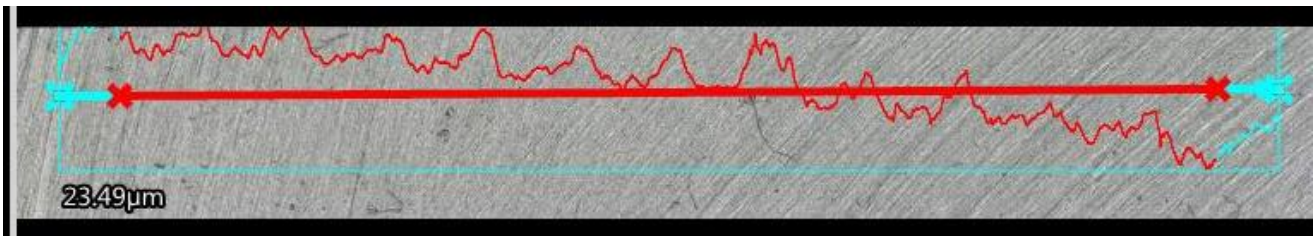

Fig. 12. Method of determining surface roughness on the line

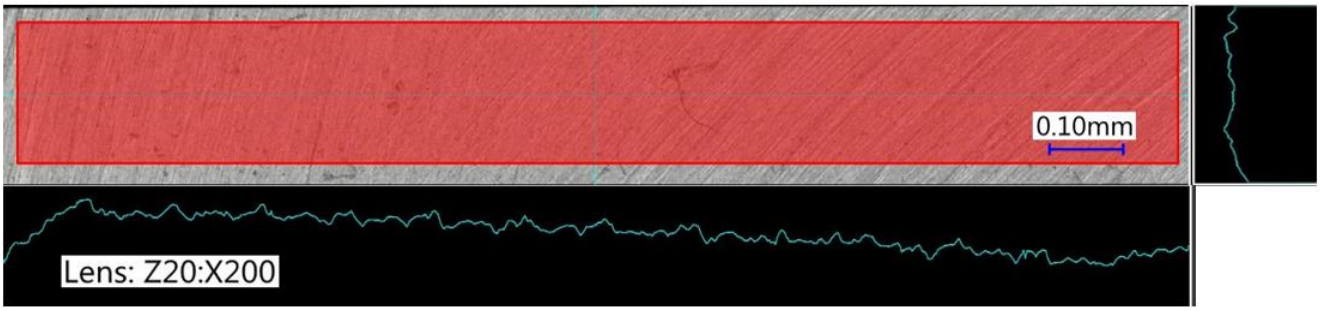

Fig. 13. Method of determining surface roughness on a surface

The surface roughness is not constant over the entire surface of the specimens which is related to the manual surface preparation process. The measurement values are shown in Table 5.

It can be observed that surfaces on which primer has been applied are smoother - they are characterized by less surface roughness. Primer gets into the recesses, leveling out material defects and easing the even distribution of adhesive layer over the entire surface.

Table 5. Surface roughness measurement values

Specimen no.	Surface preparation method	Ra [µm]	Rz [µm]	Sa [µm]	Sz [µm]
1	None	3.11	18.72	3.66	35.58
2	Primer	3.12	16.43	3.84	23.17
3	Grinding	6.13	35.92	6.62	69.72
4	Grinding + Primer	7.83	43.07	8.64	58.40
5	Sandblasting	11.37	53.58	13.80	92.68
6	Sandblasting + Primer	11.56	55.87	13.72	93.93

3. Numerical simulations

In order to analyze the stress distribution in a specimen with a hole without and after repair, numerical simulations were performed using the CAE program Ansys Workbench 2021R2. The *Static Structural* calculation module was used for this.

The *Engineering Data* program library was used to define material properties. The parameters of three materials were used for the simulation, which are shown in Tables 6 and 7. The given nonlinear properties of the aluminum alloy of the plate and the adhesive were defined as multilinear and bilinear, respectively. The parameters of the glass composite were defined as orthrotropic properties. The material data were determined experimentally using a specimen of the experimental material. For the purpose of calculation the properties of the material was homogenized.

Table 6. Material parameters in the nonlinear range of each material

Material name	Young's Modulus [GPa]	Poisson's Ratio [-]	Yield Strength [MPa]	Tangent Modulus [MPa]	Plastic Strain [-]	Stress [MPa]
AW 2024T3 NL	71.000	0.3	-	-	0	330.00
					0.0098	348.45
					0.0196	370.00
					0.0385	410.80
					0.0741	468.72
					0.1071	507.36
					0.1379	540.56
DP 420	2.083	0.35	24.00	325.00	-	-

Table 7. Material parameters of orthrotropic glass composite

Material name	Young's Modulus [GPa]			Poisson's Ratio [-]			Shear Modulus [GPa]		
Direction	X	Y	Z	XY	YZ	XZ	XY	YZ	XZ
Glass composite	15	15	5	0.04	0.3	0.3	3	2.2	2.2

In the *Geometry* module, the geometry of the specimen model was defined (Fig. 14). The model consists of an 80x150x2 mm (width, length, thickness) element with a 20 mm diameter hole - the defined specimen is shorter than the specimen used in the experiment due to the fact that the surface of the specimen located in the jaws of the testing machine of the clamping area of the grips was not included. An insert was modeled in the hole with dimensions 19,9 mm. A adhesive joint with a diameter of 70 mm and a thickness of 0.12 mm and a composite patch with a diameter of 70 mm and a thickness of 2 mm were also modeled.

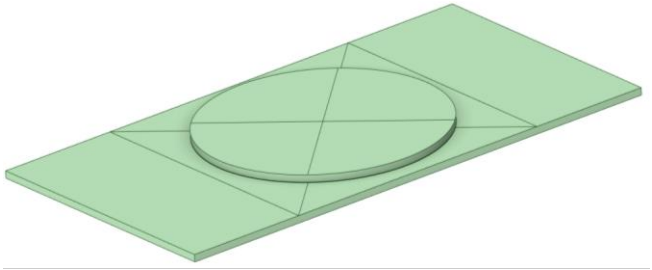

Fig. 14. Repair node model in the Geometry module

Using the *Contacts* function, the types of contacts occurring between the various elements of the model were defined to replicate the relationships that exist

between them. *Frictional* type contacts with a factor of 0.1 were defined between the insert and the plate - Fig. 15. *Bonded* type contacts were defined between the adhesive and the patch, the adhesive and the plate, and the adhesive and the insert - Fig. 16.

Discretizations of the model were performed using the Mesh function. In the mesh parameters for the entire model, the Mesh elements were given a size of 2 mm. The Multizone function with Hexa properties was used to define the type of mesh elements, which defines a hexagonal mesh type for the model. The Edge Sizing function was also used, and an element size of 1 mm was set at the edge of the hole - Fig. 17. After the geometry was discretized, a model consisting of 4289 elements and 31162 nodes of Hex20 type was obtained. The computational mesh is shown in Fig. 18.

The quality of the mesh near the hole was checked using the Element Quality function. The results of the analysis are shown in Fig. 19. The analysis of the quality of the mesh shows that it is correctly defined. Elements with values close to unity define the best quality of the computational mesh.

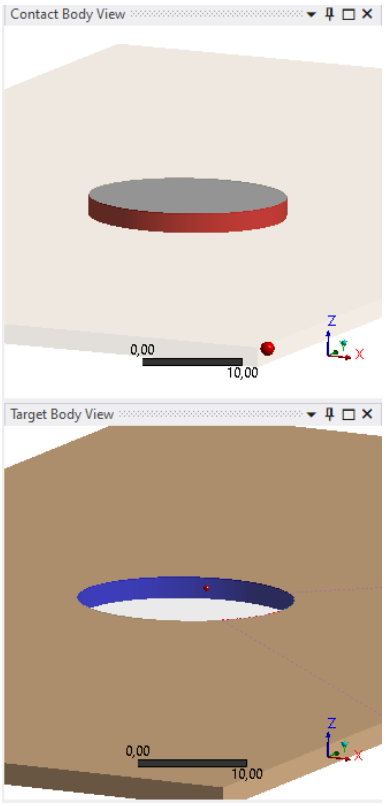

Fig. 15. Example of Frictional type of contact: insert-plate

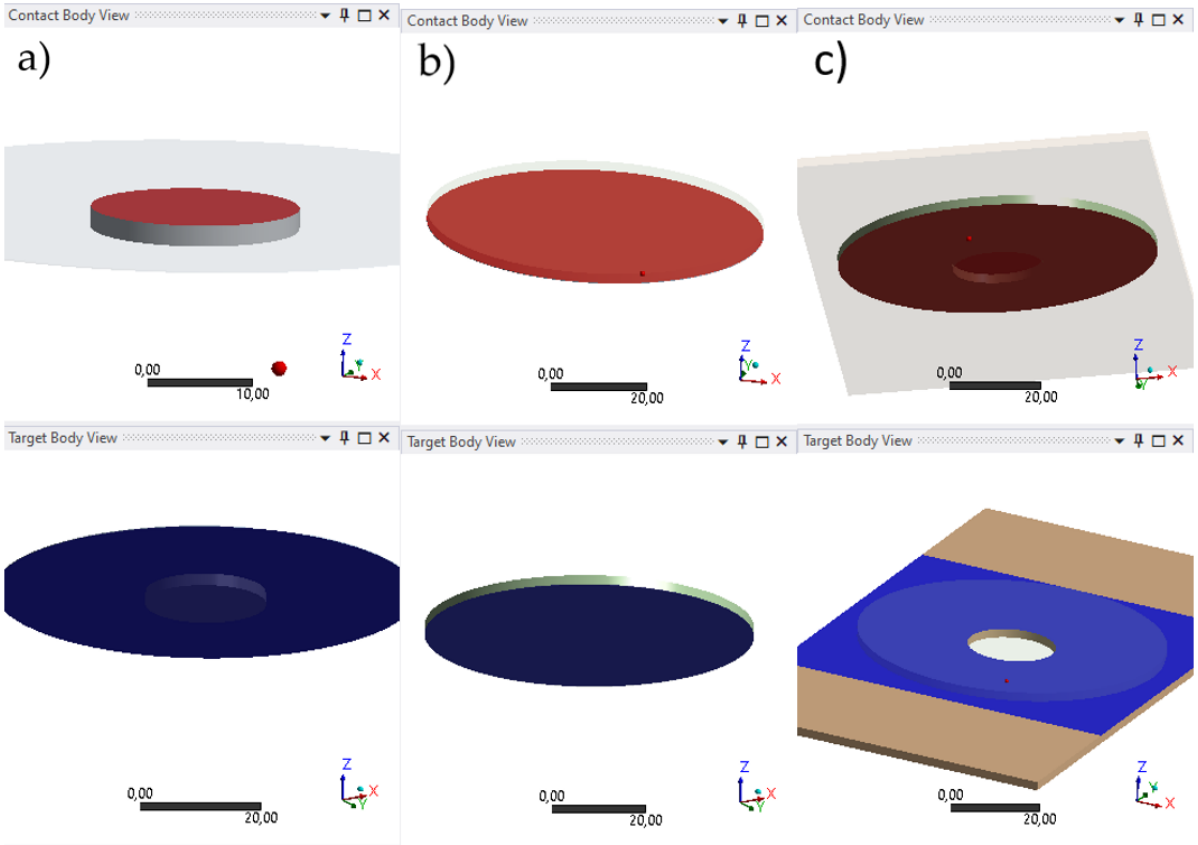

Fig. 16. Examples of Bonded type of contact: insert-adhesive (a), adhesive-bonded (b), adhesive-plate (c)

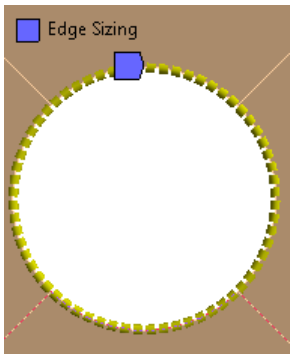

Fig. 17. Using the Edge Sizing function to thicken the mesh around the hole

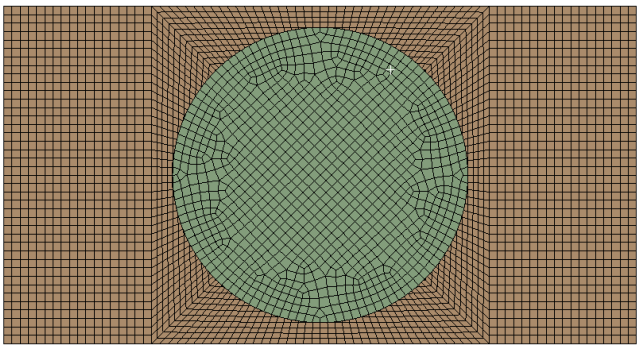

Fig. 18. Discretized numerical model

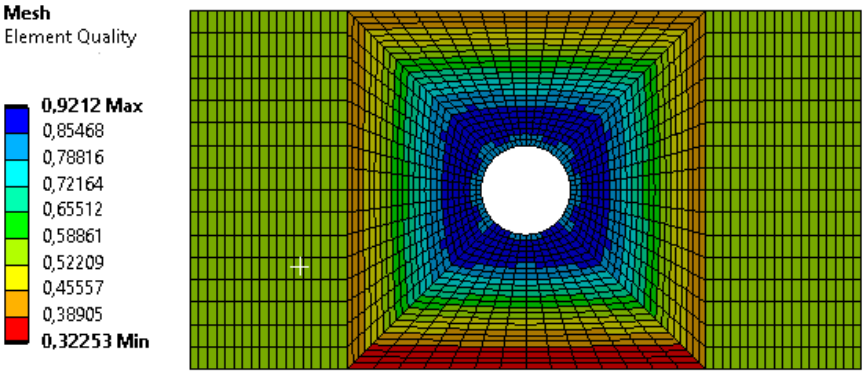

Fig. 19. Quality analysis of mesh elements around the hole

The boundary conditions were given using the *Static Structural* function. The computational model replicate the loading conditions of the specimen in the testing machine - Fig. 20. One side - was fixed using the *Fixed Support* function. All six degrees of freedom were taken away from the nodes $-D_X; D_Y; D_Z = 0$, $R_X; R_Y;\ R_Z = 0$. For the second side, a *Force* load of 60 kN in the Y direction was defined. The value of the destructive force of such a specimen was determined in the experimental part. The second side was also fixed using the *Displacement* function on two directions $-D_X; D_Z = 0;\ D_Y = Free$.

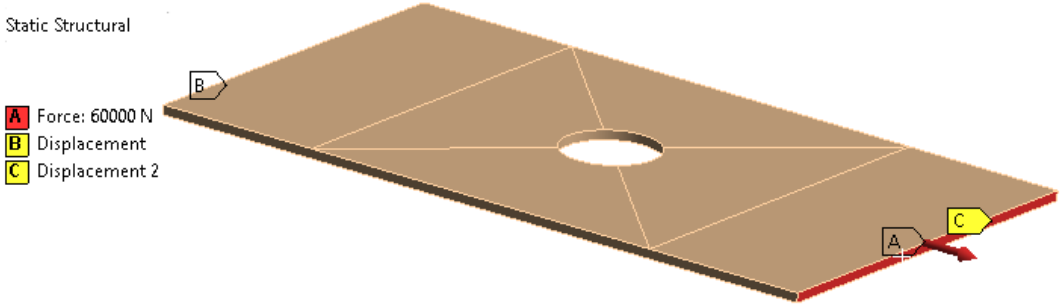

Fig. 20. The boundary conditions of the model (A - force, B and C - restraint)

Simulation results

Strength calculations were performed using the Solution function. The *von-Mises* stress in the repair plate is shown in Fig. 21. The largest *Equivalent Plastic Strain* in the model has a value of 0.247 and occurs around the hole in the adhesive layer - Fig. 22.

Analyzing the reduced von-Mises stresses in the adhesive bond - Fig. 23 - the occurrence of stress concentration phenomenon and failure stresses of the adhesive layer was observed in the vicinity of the hole. The distribution of von-Mises stresses in the patch is shown in Fig. 24.

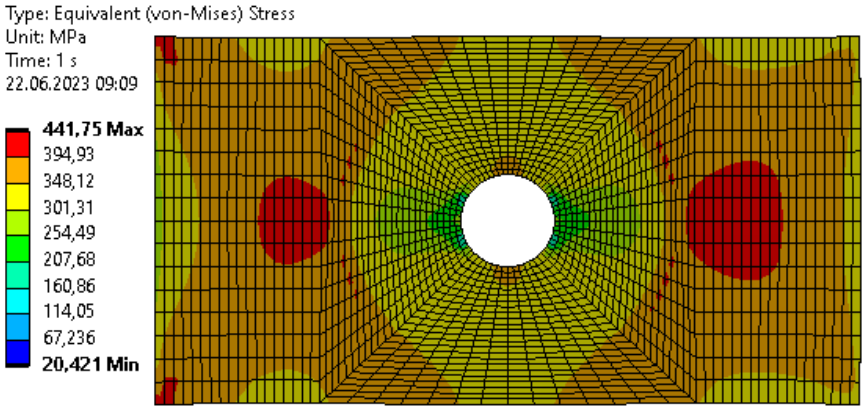

Fig. 21. Von-Mises stress map - plate

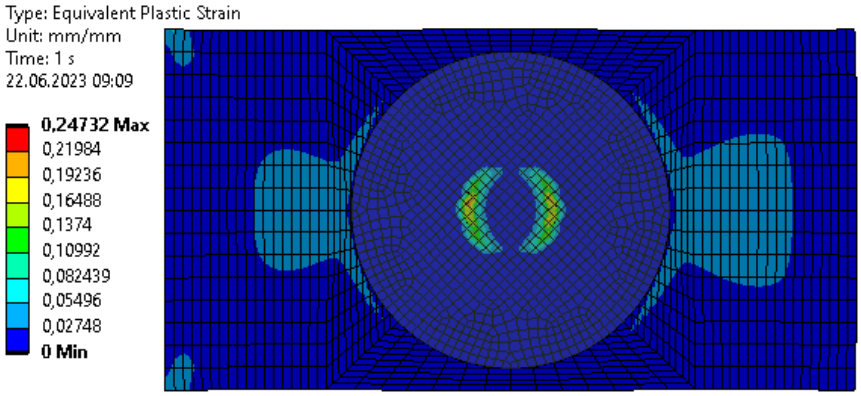

Fig. 22. Equivalent Plastic Strain map of the model

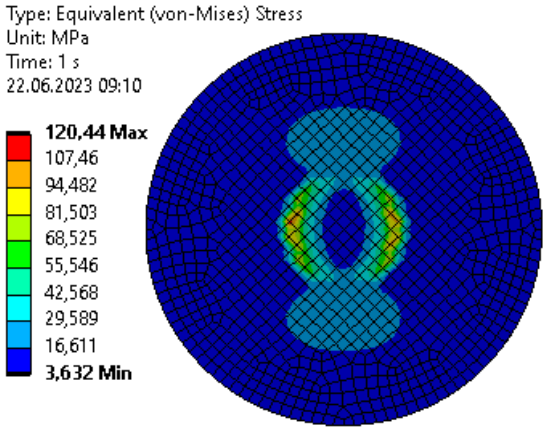

Fig. 23. Von-Mises reduced stress map – adhesive layer

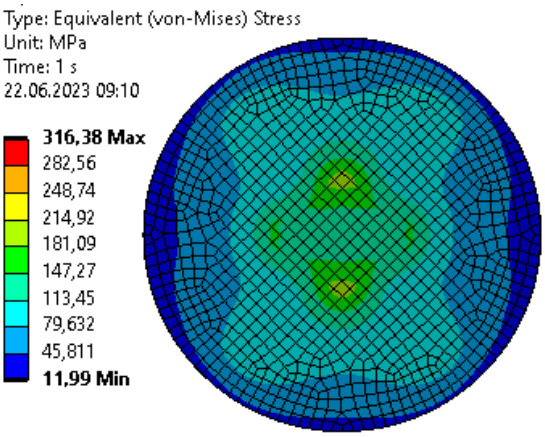

Fig. 24. Von-Mises reduced stress map - patch

Calculations were also carried out for a plate with a hole without a repair. The material parameters, geometry and boundary conditions are analogous to the previous model. The load for this design case is equal to 50 kN (the value obtained from experimental tests) (Fig. 25).

Table 8 summarizes the obtained results of the numerical analyses.

Analyzing the obtained results, a decrease in stresses in the plate was observed after the repair. In the adhesive layer, there are stresses with values exceeding the cohesive strength of the adhesive - which may indicate the destruction of the joint in the original construction.

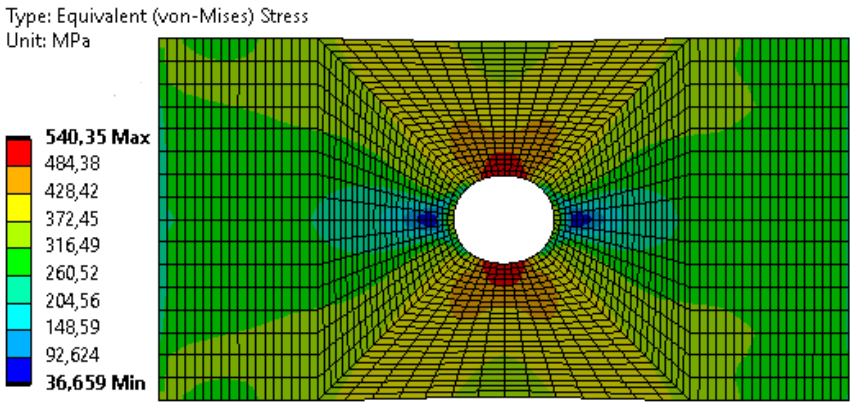

Fig. 25. Von-Mises stress map for the damaged plate

Table 8. Results of numerical simulations for two models (maximum value of Von Mises stresses)

Model type	Von-Mises [MPa]		
	Plate	Patch	Adhesive layer
Damage	540.35	-	-
Repaired	441.75	316.38	120.44

4. Conclusions

Based on the experimental tests and numerical simulations, the following conclusions were defined:

In order to prepare an effective repair node, it is necessary to select, among other things, a suitable adhesive and a method of preparing the surfaces to be joined. In our study, the most favorable results were obtained by preparing the surface by grinding and then using primer. After using primer, the load capacity of lap joints increased by 57%.

The study showed that the use of primer also affects the surface roughness. The parameters defining surface roughness after primer use are lower which is due to the filling of cavities in the material. Too much surface roughening is unfavorable because it lowers the contact area between the adhesive and the material.

Composite surfaces have potentially higher adhesion than surfaces of metal parts. By using an effective method to prepare the surface of the metal part for bonding, a solution can be obtained in which the adhesive strength of the joint is higher than the cohesive strength of the composite part.

Based on numerical calculations, it was found that the use of an adhesive overlay significantly reduces the phenomenon of stress concentration around the hole.

Bibliography

1. Starke E.A. Jr., Staley J.T. 2011. Chapter 24: Application of modern aluminum alloys to aircraft. Fundamentals of Aluminium Metallurgy. *Production, Processing and Applications*. Pages 747-783. Woodhead Publishing Series in Metals and Surface Engineering.
2. Baker Alan A., Wang John. 2018. Chapter 6: Adhesively Bonded Repair/Reinforcement of Metallic Airframe Components: Materials, Processes, Design and Proposed Through-Life Management. *Aircraft Sustainment and Repair*. Pages 191-252. Butterworth Heinemann.
3. Baker Alan A., Jones Rhys A.C. 2012. "Bonded Repair of Aircraft Structures". *Springer Science & Business Media*.
4. Baker A.A. 2002. Chapter 1: Introduction and Overview. *Advances in the bonded composite repair of metallic aircraft structure – Volume 1*. Pages 1-18.
5. Shang X., Marques E.A.S., Machado J.J.M., Carbas R.J.C., Jiang D., da Silva L.F.M. 2019. "Review on techniques to improve the strength of adhesive joints with composite adherends". *Composite Part B: Engineering* 177.
6. Kweon J.H., Jung J.W., Kim T.H., Choi J.H., Kim D.H. 2006. "Failure of carbon composite-to-aluminum joints with combined mechanical fastening and adhesive bonding". *Composite Structures* 75: 192–198.
7. Jeevi G., Nayak S.K., Abdul K.M. 2019. "Review on adhesive joints and their application in hybrid composite structures". *Journal of Adhesion Science and Technology* 33 (14).
8. Zitoune R, Collombet F. 2007. "Numerical prediction of the thrust force responsible of delamination during the drilling of the long-fibre composite structures". *Composite Part A: Applied Science and Manufacturing* 38: 858–866.
9. Davim J.P., Reis P., Antonio C.C. 2004. "Drilling fiber reinforced plastics (FRP) manufactured by hand lay-up: influence of matrix (Viapal VUP 9731 and ATLAC 382-05)". *Journal of Materials Processing Technology* 155––156 : 1828–1833.
10. Kupski J., Teixeira de Freitas S. 2021. "Design of adhesively bonded lap joints with laminated CFRP adherends: Review, challenges and new opportunities for aerospace structure". *Composite Structures* 268 : 113923.

11. Yudhanto A., Alfano M., Lubineau G. 2021 "Surface preparation strategies in secondary bonded thermoset-based composite materials: A review". *Composites Part A: Applied Science and Manufacturing* 147 : 106443.
12. Gary C.W. 2021. Chapter 4: Surface pretreatments for optimized adhesive bonding. Adhesive Bonding (Second Edition) Science, Technology and Applications. *Woodhead Publishing Series in Welding and Other Joining Technologies*. Pages 109-132.
13. Loutas T.H., Sotiriadis G., Bonas D., Kostopoulos V. 2019. "A statistical optimization of a green laser-assisted ablation process towards automatic bonded repairs of CFRP composites". *Polymer Composites* 40 (8).
14. Dillingham R.G., Oakley B.R., Dan-Jumbo E., Baldwin J., Keller R., Magato J. 2014. "Surface treatment and adhesive bonding techniques for repair of high-temperature composite materials". *Journal Composite Materials*, 48 (7).
15. Baker A.A., Jonse R. 2002. "Advances in the bonded composite repair of metallic aircraft structure. Volume 1". *Elsevier Applied Science Publishers*.
16. Banea M.D., Da Silva L.F. 2009. Adhesively bonded joints in composite materials: an overview. *Proceedings of the Institution of Mechanical Engineers, Part L: Journal of Materials: Design and Applications* 223:1–18.
17. Dillingham R.G. 2013. "Qualification of surface preparation processes for bonded aircraft repair". *BTG Labs*. 2013.
18. Hamill L., Nutt S. 2018. "Adhesion of metallic glass and epoxy in composite-metal bonding". *Composites Part B: Engineering* 134, Pages 186-192.
19. Li S., Sun T., Liu Ch., Yang W., Tang Q. 2018. "A study of laser surface treatment in bonded repair of composite aircraft structures". *The Royal Society Publishing* 18 (3).
20. Chester R. 2002. Chapter 2: Materials Selection and Engineering. *Advances in the bonded composite repair of metallic aircraft structure – Volume 1*. Pages 19-40.
21. Andrew J.J., Srinivasan S.M., Arockiarajan A. 2019. "Influence of patch lay-up configuration and hybridization on low velocity impact and post-impact tensile response of repaired glass fiber reinforced plastic composites". *Journal Composite Materials*, 53 (1), pp. 3-17.
22. Zhou W., Ji X., Yang S., Liu J., Ma L. 2021. "Review on the performance improvements and non-destructive testing of patches repaired composites". *Composite Structures* 263. 113659.
23. Yala A.A., Megueni A. 2009. "Optimisation of composite patches repairs with the design of experiments method". *Materials and Design* 30 (1), pp. 200-205.
24. Bouanani M.F., Benyahia F., Albedah A., Aid A., Bouiadjra B., Belhouari M., Achour T. 2013. "Analysis of the adhesive failure in bonded composite repair of aircraft structures using modified damage zone theory". *Materials and Design* 50, pp. 433-439